

# Improved atmospheric mapping functions for VLBI and GPS

A. E. Niell

MIT Haystack Observatory, Westford, MA 01886, U.S.A.

(Received January 17, 2000; Revised June 26, 2000; Accepted July 2, 2000)

New mapping functions based on *in situ* meteorological parameters have been developed for calculating the radio path length through the atmosphere at elevations down to  $3^\circ$ . The hydrostatic component of the mapping function is related to the geopotential height of the 200 mb isobaric pressure level above the site and provides a factor of two improvement in accuracy and precision over previous hydrostatic mapping functions at mid-latitudes. The wet component of the mapping function is calculated from the vertical profile of wet refractivity at the site but will provide an improvement of only about twenty-five percent. However, since the effect of known errors in the hydrostatic mapping function dominates that from the wet component, except near the equator, implementation of these mapping functions should reduce the contribution of the atmosphere to errors in estimates by VLBI and GPS of both the vertical component of site position and the radio propagation delay due to water vapor in the atmosphere.

## 1. Introduction

In space geodetic measurements by Very Long Baseline Interferometry (VLBI) and the Global Positioning System (GPS) a primary impediment to reducing the uncertainty in site position and zenith atmosphere delay is the error in characterizing the propagation delay through the atmosphere. The geometric strength of the estimation process can be improved by reducing the minimum elevation to which observations are obtained. However, any gain must be balanced against the decrease in accuracy due to the increased uncertainty in the estimated atmosphere parameters.

For space geodesy applications the atmosphere is characterized primarily by two mapping functions which relate the delay at the elevation of observation to the delay in the zenith direction. (See Davis *et al.* (1985) or Niell (1996) for discussion.) There are separate mapping functions for the hydrostatic and water vapor components of the atmosphere. (The effect of azimuthal asymmetry, usually accounted for by estimating a first order horizontal gradient in the atmosphere delay, will not be discussed.)

Current mapping functions use either surface meteorology measurements and site location (Davis *et al.*, 1985 (CFA2.2); Herring, 1992 (hereafter referred to as MTT); and Ifadis, 1986) or only site location and time of year (Niell, 1996 (NMF)). Unless correlations among surface properties can be found that have not yet been explored, any improvement in the mapping functions appears to require information on the actual state of the atmosphere. One source of atmospheric data that might be available with a reasonably uniform temporal and spatial distribution is a global meteorological weather analysis or prediction. The information needed to calculate the mapping functions would be obtained by interpolating from the grid points of the analysis to the position of the

site. If suitable mapping functions can be derived based on such global analyses, which have grid spacings of a few degrees, then more accurate and denser (in either space or time) analyses might provide even greater accuracy.

## 2. Mapping Function Derivation

The mapping function,  $m(e)$ , is defined as the ratio of the electrical path length (also referred to as the delay) through the atmosphere at geometric elevation,  $e$ , to the electrical path length in the zenith direction. For a planar atmosphere the ratio would be given by  $1/\sin(e)$ . As the ratio of the thickness of the atmosphere to the radius of the earth decreases, the atmosphere appears more planar. Thus a possible proxy for the mapping function is some quantity that is a measure of the thickness of the atmosphere.

The 'true' mapping functions, which serve as the standard of comparison for the models, are calculated by raytracing through the atmosphere using the state given by vertical profiles of the pressure, temperature, and relative humidity obtained from radiosonde profiles. Spherical symmetry is assumed.

The mapping function is conveniently separated into two components, the hydrostatic and the wet (Davis *et al.*, 1985).

### 2.1 Hydrostatic mapping function

The zenith hydrostatic delay is proportional to the integral of the density of the hydrostatic part of the atmosphere. Thus, because the atmosphere is very close to hydrostatic equilibrium, a contour of constant pressure (isobar) provides the height above the geoid of a constant delay, and these heights might be expected to serve as the parameter needed for the hydrostatic mapping function.

This proposal was tested using data from the year 1992. Radiosonde data were obtained from the National Center for Atmospheric Research for twenty-six sites. The sites were chosen for their proximity to the antennas of the global geodetic VLBI network. The gridded model data were taken

from the re-analysis of the Goddard Space Flight Center Data Assimilation Office (DAO) (Schubert *et al.*, 1993). The radiosonde data were used to determine the “true” mapping functions for the twenty-eight sites, and the DAO data provided the meteorological parameters on a  $2^\circ$  by  $2.5^\circ$  grid in latitude and longitude. For determining the hydrostatic mapping function the parameter extracted from the DAO data set was the geopotential height,  $z$ . Figure 1 presents the radiosonde-derived hydrostatic mapping functions at  $5^\circ$  and the 200 mb geopotential heights for ALB for 1992 December. The 200 mb level showed the highest correlation with the mapping function at  $5^\circ$  and was the minimum pressure level that seemed to be widely available for use by the global community at the time that the coefficients of the hydrostatic mapping function were being evaluated.

The form adopted for the mapping functions is the continued fraction with three coefficients (see Niell (1996) for additional discussion):

$$m(e) = \frac{1 + \frac{a}{1 + \frac{b}{1 + c}}}{\sin(e) + \frac{a}{\sin(e) + \frac{b}{\sin(e) + c}}}$$

where  $e$  is the geometric elevation of the observation. The objective is to determine the functional form of the coefficients,  $a$ ,  $b$ , and  $c$ . From the discussion above they are related to the isobaric height, but they may also be a function of the site location.

The following procedure was used to evaluate the coefficients. All of the profiles ( $\sim 730$ ) for each of the twenty-eight sites were raytraced for nine elevations from  $90^\circ$  down to  $3^\circ$ . For each profile the coefficients  $a$ ,  $b$ , and  $c$  that best fit the ratios of the delays at the nine elevations to the

zenith delay were estimated by least squares. From the mean geopotential height over the year for each site a reference geopotential surface that is a function of latitude of the form  $\cos(2 * \text{latitude})$  was determined. A latitude dependence is expected since the temperature profile that results in the same pressure and geopotential height at high latitudes will be quite different from the corresponding profile at the equator. Each of the coefficients was then expanded to second order in  $z - z_{ref}$  and  $\cos(2 * \text{latitude})$ . For the  $a$  coefficient, all but the  $z^2$  term were found to be significant. For  $b$  only the mean value is used, and  $c$  is linear in  $\cos(2 * \text{latitude})$ . The functional form,  $\cos(2 * \text{latitude})$ , is empirical and is suggested by symmetry about the axis of rotation and about the equator. This hydrostatic mapping function will be referred to as IMFh.

## 2.2 Wet mapping function

Attempts to determine a height-dependent wet mapping function based on the vertical distribution of water vapor content were unsatisfactory. Instead an algorithm was developed based on integrating the wet refractivity along the geometric path for a spherical atmosphere at a low elevation. The elevation adopted was  $3^\circ$ , which is the lowest value for which the radiosonde data were raytraced to calculate the mapping functions. This procedure produced a “wet parameter” for the profile of wet refractivity determined from the temperature and relative humidity at the height of each pressure level. Following the same procedure as described above for the hydrostatic mapping function, coefficients for a wet mapping function were determined. The model is considerably simpler than for the hydrostatic mapping function: the coefficients,  $a$ ,  $b$ , and  $c$ , are linear functions of only the single “wet parameter”. This wet mapping function will be referred to as IMFw.

## 3. Comparison with Current Mapping Functions

For a new model to be worth expending effort to adopt, it should offer significant improvement over existing analysis procedures. Two widely used mapping functions are MTT (Herring, 1992) and NMF (Niell, 1996). (Ifadis (1986) has comparable accuracy (Niell, 1996; Mendes, 1999) and in the comparisons would be almost identical to MTT.) NMF and MTT are among the most accurate when observations at elevation angles below  $15^\circ$  are to be included (Mendes, 1999), but they are based on very different principles, as mentioned in the introduction. These two, which contain both wet and hydrostatic components, and the proposed new mapping functions have been evaluated by comparing the values calculated at  $5^\circ$  with the wet and hydrostatic mapping functions determined by raytracing the corresponding radiosonde profile. This is a stringent test of the accuracy of the mapping functions since the lowest elevations have the largest effect on the geodetic estimation. It is a sufficient test because the continued fraction calculated with the fitted coefficients agreed with the original raytraced mapping function at each elevation to better than one millimeter in path length.

The means and standard deviations of the differences between the analytic mapping functions and the mapping functions obtained by raytracing the radiosonde profiles from the twenty-six sites were calculated for all good profiles for an

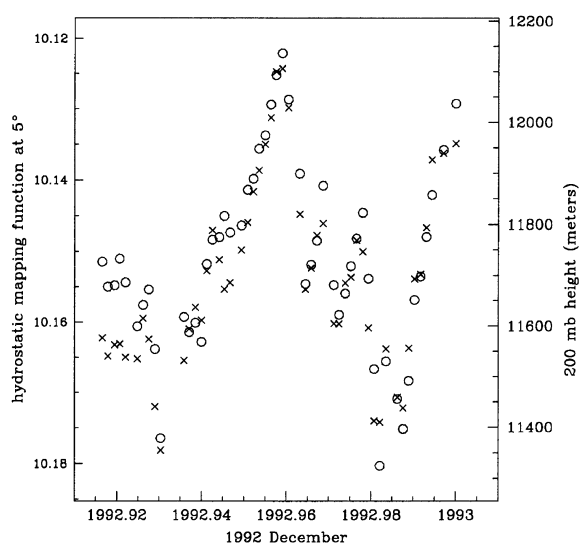


Fig. 1. The hydrostatic mapping functions from radiosonde data at the site ALB (circles—left axis) and the geopotential height of the 200 mbar surface interpolated to the same latitude and longitude (crosses—right axis) for the month of December 1992.

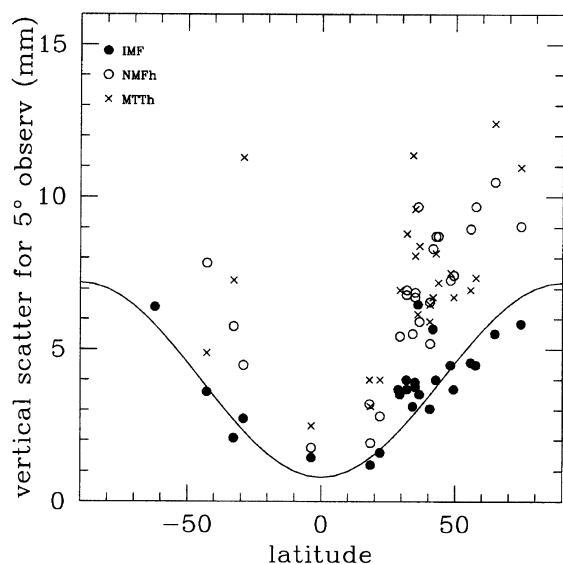


Fig. 2. Standard deviation of apparent height calculated from the differences between the raytraced radiosonde profiles and the analytic hydrostatic mapping function calculations using MTTh, NMFh, and that based on the 200 mb isobars from the DAO assimilated data set (IMFh) (MTTh—cross; NMFh—open circle; IMFh—filled circle).

elevation of  $5^\circ$ . In order to present the comparison in terms of geodetic results the means and standard deviations have been converted to apparent height errors assuming data were recorded down to this same elevation. For a geodetic analysis of GPS or VLBI observations in which site position, atmosphere delay, and site clocks are estimated (along with other necessary model parameters), the error in height appears as approximately one-third of the path length error at the lowest observed elevation (MacMillan and Ma, 1994; Niell, 1996). Similarly, due to the correlation of the atmosphere delay and the site height of approximately  $-0.4$ , the error in estimated troposphere zenith delay is approximately one-tenth of the path length error at the lowest observed elevation. These conversion factors are used below for relating the standard deviations of the mapping functions to uncertainties in height and in zenith delay. Although the factors themselves have variations of up to 30% (MacMillan and Ma, 1994), the relative contribution of wet and hydrostatic, or of two different hydrostatic or wet, mapping functions is correct.

### 3.1 Hydrostatic mapping function

The standard deviations of the height error calculated for the hydrostatic mapping functions are shown in Fig. 2 for twenty-six sites. For mid-latitudes the mapping function based on the 200 mb isobars will reduce the height standard deviation due to atmosphere estimation by a factor of about two compared to NMF and MTT. The solid line indicates a  $\cos(2 \times \text{latitude})$  dependence. The largest errors are at higher latitudes due, presumably, to the greater variability of the atmosphere. The differences of IMFh and NMFh with respect to the raytraced mapping functions are shown in Fig. 3 for ALB in the northeast United States. An important improvement of IMFh is the reduction of the seasonal error, both in scatter and bias.

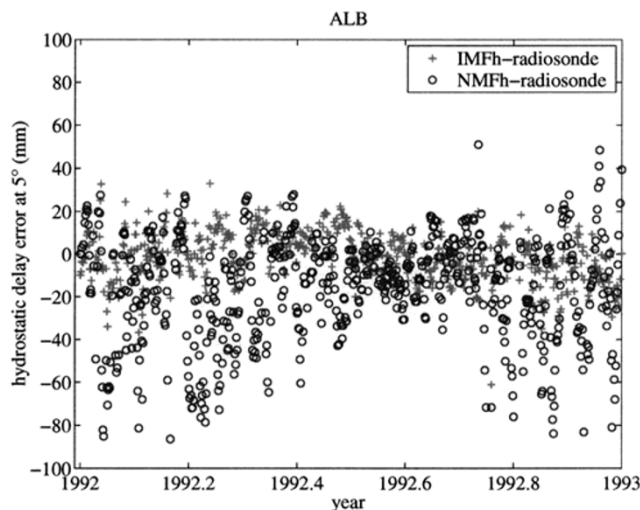


Fig. 3. Differences between hydrostatic mapping functions at  $5^\circ$  and those obtained from raytracing the radiosonde profiles for the site ALB in the northeast United States for 1992 (NMFh—open circle; IMFh plus sign).

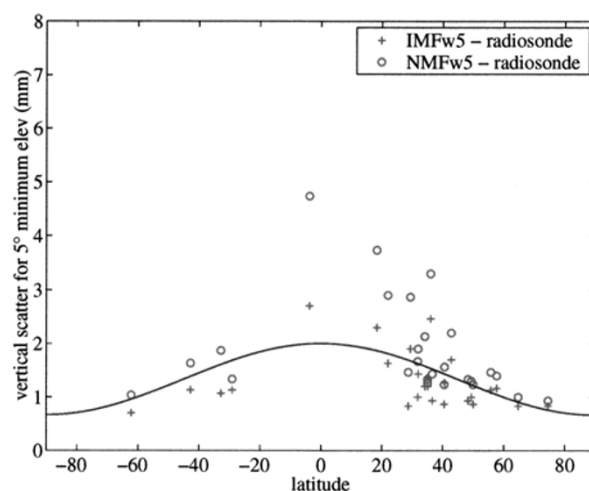


Fig. 4. Standard deviation of apparent height calculated from the differences between the raytraced radiosonde profiles and the analytic wet mapping function calculations (NMFw5—open circle; IMFw5—plus sign).

### 3.2 Wet mapping function

The standard deviations of the height error calculated for the wet mapping functions are shown in Fig. 4. In this case the parameters of the mapping function are not determined from the gridded data but from the radiosonde profiles themselves. The resulting improvement indicated in the figure is thus an upper limit since the gridded data will be less representative of the local profile and will most likely have poorer vertical resolution. The improvement that may be realized for the wet mapping function is significantly less than for the hydrostatic function, averaging about twenty-five percent.

It is important to note that the magnitude of the wet delay standard deviation depends on both the mapping function error and the amount of water vapor. Fortaleza, for example, at a latitude of  $-2^\circ$ , has one of the three lowest standard deviations of mapping function difference, but it has the largest

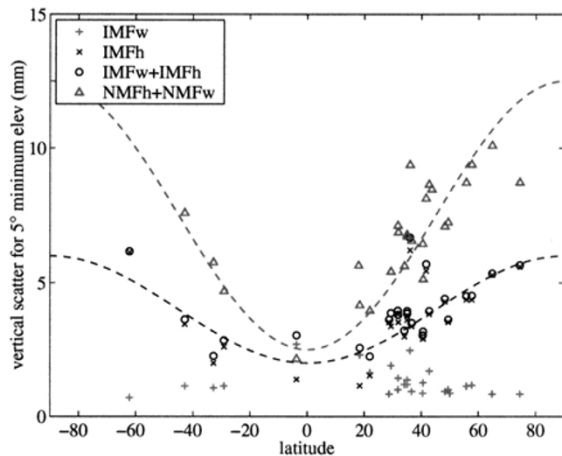


Fig. 5. Standard deviation of apparent height for the combined errors of the hydrostatic and wet mapping functions. Except at very low latitudes the error due to the wet mapping function is insignificant (IMFw—plus sign; IMFh—cross; IMFw + IMFh—open circle; NMFw + NMFh—asterisk).

standard deviation of delay error.

#### 4. Combined Mapping Function Error

Which mapping function error is most important? In Fig. 5 the standard deviations of the inferred height errors for the hydrostatic and wet components have been combined quadratically. The resulting total height error is shown for the proposed new mapping functions and for NMF. Contrary to the expectation that water vapor is the major source of error, the height error is dominated by the hydrostatic component, except possibly near the equator. Thus it is clear that an improvement in the hydrostatic component will have the larger impact on improving the measurement of height and of atmosphere delay by VLBI and GPS.

#### 5. Possible Implementation

Gridded isobaric height data, as used for IMFh, and the corresponding profile information on height and water vapor content needed for IMFw, are publicly available from several of the major meteorological analysis centers at time intervals as short as six hours on a global grid. The differences shown in Fig. 3 for ALB are for twice-daily observations. However, by using data every six hours, the error in the estimate of the vertical due to interpolation of the input data will be less than 1 mm for observations down to an elevation of 5°.

For efficient use of the global resources it is desirable that one or more of the meteorological analysis centers make the gridded data available for download by the space geodesy data centers. The analysis centers or individual analysts can then retrieve the meteorological data.

The amount of data that are needed for the hydrostatic mapping functions will be significantly less than for the wet mapping functions. For the hydrostatic mapping function only one parameter, the height of one isobaric level, is needed at each of the grid points. For the wet mapping function several values (e.g. geopotential height or pressure, temperature, and a measure of water vapor, such as relative humidity)

are required at as many levels as are present. Since improving the hydrostatic mapping function provides a significantly greater contribution than that of the wet mapping function, one option for operations is to use the new IMFh but continue with NMFw for the partial derivative of the atmosphere estimation. For highest accuracy, however, both of the new mapping functions should be used since the wet mapping function serves as the partial derivative for estimating the zenith wet delay.

#### 6. Implications

In general changes are made to an analysis model in order to improve the accuracy and precision of the estimated parameters. It is therefore important that all data be evaluated with the same model to avoid systematic changes that might be interpreted as temporal variation. For example, changing the minimum elevation of data included in a VLBI or GPS solution can introduce a relative bias in the mean vertical component of station position (see MacMillan and Ma (1994) or Niell (1996) for the effect of different mapping functions on VLBI data).

For the twenty-six sites investigated the biases in height that would be introduced by the new hydrostatic mapping function for 5° minimum elevation of observation lie between -1 and +4 millimeters relative to the heights that would be obtained using the radiosonde-based values. The height biases for NMFh range from -6 mm to +6 mm, so the improvement is significant.

**Acknowledgments.** I thank Michelle Machacek for decoding the DAO Assimilated data sets and for significant contributions to the programs on which these results are based. I am grateful to Dr. Seiichi Shimada and to the Government of Japan through the National Research Institute for Earth Science and Disaster Prevention, Science and Technology Agency, for a research award. This work was supported by NASA grants NAS5-99198 and NAG5-6063.

#### References

- Davis, J. L., T. A. Herring, I. I. Shapiro, A. E. E. Rogers, and G. Elgered, Geodesy by radio interferometry: Effects of atmospheric modeling errors on estimates of baseline length, *Radio Sci.*, **20**, 1593–1607, 1985.
- Herring, T. A., Modelling atmospheric delays in the analysis of space geodetic data, in *Symposium on Refraction of Transatmospheric Signals in Geodesy*, edited by J. C. DeMunk and T. A. Spoelstra, Netherlands Geodetic Commission Series No. 36, pp. 157–164, 1992.
- Ifadis, I., The atmospheric delay of radio waves: modeling the elevation dependence on a global scale, Technical Report No. 38L, School of Electrical and Computer Engineering, Chalmers University of Technology, Gothenburg, Sweden, 1986.
- MacMillan, D. S. and C. Ma, Evaluation of very long baseline interferometry atmospheric modeling improvements, *J. Geophys. Res.*, **99**(B1), 637–651, 1994.
- Mendes, V. B., Modeling the neutral-atmosphere propagation delay in radiometric space techniques, Ph.D. Dissertation, Department of Geodesy and Geomatics Engineering Technical Report No. 199, University of New Brunswick, Fredericton, New Brunswick, Canada, 353 pp, 1999.
- Niell, A. E., Global mapping functions for the atmosphere delay at radio wavelengths, *J. Geophys. Res.*, **100**, 3227–3246, 1996.
- Schubert, S. D., J. Pjaendtner, and R. Rood, An assimilated data set for Earth science applications, *B. A. M. S.*, **74**, 2331–2342, 1993.